MedChemComm

Accepted Manuscript

This article can be cited before page numbers have been issued, to do this please use: K. Hu, C. Liu, J. Li and F. Liang, *Med. Chem. Commun.*, 2018, DOI: 10.1039/C8MD00223A.




ROYAL SOCIETY OF CHEMISTRY

rsc.li/medchemcomm

View Article Online
DOI: 10.1039/C8MD00223A

Journal Name

ARTICLE

# Copper(II) complexes based on quinoline derived Schiff-base ligands: synthesis, characterization, HSA/DNA binding ability, and anticancer activity

Received 00th January 20xx,
Accepted 00th January 20xx

DOI: 10.1039/x0xx00000x

www.rsc.org/

Kun Hu, *[a] Chensi Liu,[a] Jingui Li[a] and Fupei Liang*[a,b]

Three copper(II) complexes[Cu(L1)(NO3)2] (**C1**), [Cu(L2)Cl2] (**C2**) and [Cu(L2)$SO_4$]2·$H_2O$ (**C3**) were designed and synthesized by reaction of $Cu(NO_3)_2·3H_2O$, $CuCl_2·2H_2O$ and $CuSO_4·5H_2O$ with a quinoline derived Schiff base ligand L1 or L2 prepared by condensation of quinoline-8-carbaldehyde with 4-amino-benzoic acid methyl ester or 4-amino-benzoic acid ethyl ester (benzocaine). The efficient bindings of the **C1**-**C3** with human serum albumin (HSA) and calf thymus DNA (CT-DNA) were analyzed by spectroscopy and molecular docking. These complexes could significantly quench the fluorescence of HSA through static quenching process, and hydrophobic interaction with HSA through sub domain IIA and IIIA cavity. Meanwhile, the complexes could bind to DNA via intercalative mode, and they fit well into the curved contour of the DNA target into the minor groove region. Furthermore, the interaction ability of the Cu(II) complexes with HSA/DNA was more than their corresponding ligand. Interestingly, **C1**-**C3**, especially **C3** exhibited more cytotoxic to HeLa cells compared to normal HL-7702 cells and other three tumor cell lines (Hep-G2, NCI-H460, and MGC80-3). Moreover, their cytotoxicity toward the HeLa cell lines was 1.9-3.5-fold more potent than cisplatin. Further studies indicated that these complexes arrested cell cycle in G0/G1 phase and promoted tumor cell apoptosis via reactive oxygen species (ROS)-mediated mitochondrial pathway.

## 1. Introduction

With the development of medicinal inorganic chemistry, especially the anticancer activity of cisplatin being found, metal-based drugs have been placed in the frontline in the fight toward cancer.[1] Among these bio-essential metals, the homeostasis and metabolism of copper are important to all kinds of human cancers, and copper levels in tumor tissue of cancer patients significantly elevated compared to normal tissue.[2] So, cancer cells may represent a suitable and selective target for copper-based agents.[3] The copper also alters cancer cells metabolism and exhibits differential response to tumor cells compared with normal cells, which endowed copper complexes essential antineoplastic characteristics. Therefore, copper complexes showed encouraging perspectives and are considered as promising alternatives to platinum drugs in this field.[1,4,5]

Recent literature revealed that the activity of metal-based anticancer agents was the effect of the ligand framework. Because the organic ligand could regulate metal absorption, distribution, and metabolism in biological systems, and thus reduce toxic side effects, improve efficiency, enhance delivery, and provide better activities in drug resistance cells.[6] Thus, the ligand introduced was crucial for the metal-based anticancer agents. As an important class of compounds, Schiff bases have drawn considerable attention due to their bioactivities, pharmacological activities and good coordination ability with metal ion.[7-9] Some Schiff bases and their copper complexes have been designed and employed as very effective metal-based multiple drug resistance modulators.[10-12] Moreover, Schiff base copper complexes can also bind DNA or cause DNA damage, promote intracellular reactive oxygen species (ROS) levels, as well as the activation on the mitochondrial pathway and induce caspase-dependent apoptosis.[13, 14]

Quinoline and its derivatives, as an important class of biologically active heterocyclic compounds, exhibited various pharmaceutical activities.[15-18] In particular, quinoline scaffolds play a key role in the development of anticancer drugs because they exhibit excellent results by different mechanisms of action such as growth inhibitors by apoptosis induction, cell cycle arrest, and disruption of cell migration and inhibition of angiogenesis.[16] Copper complex based on quinoline Schiff base has been found to show significant

[a] State Key Laboratory Cultivation Base for Chemistry and Molecular Engineering of Medicinal Resources, School of Chemistry and Pharmacy, Guangxi Normal University, 15 Yucai Road, Guilin 541004, P. R. China., Fax, 086-773-2120958 ; E-mail: hukun216@163.com, fliangoffice@yahoo.com.
[b] Guangxi Key Laboratory of Electrochemical and Magnetochemical Functional Materials, College of Chemistry and Bioengineering, Guilin University of Technology, Guilin 541004, China.

Electronic Supplementary Information (ESI) available: CCDC 1587628, 1587630 and 1587631.For ESI and crystallographic data in CIF or other electronic format. See DOI: 10.1039/x0xx00000x

View Article Online
DOI: 10.1039/C8MD00223A




perspectives for anticancer therapies. For example, several quinoline-2-carboxaldehyde Schiff base copper complexes were reported and showed antiproliferative activity toward prostate cancer cells and cervical cancer cell.[19-22] Following these report, aminoquinoline Schiff base copper complexes were also synthesized and evaluated their anticancer activity.[22,23] A series of 2-oxo-1, 2-dihydroquinoline-3-carbaldehyde (2′-hydroxybenzoyl,[24] benzoyl,[25] 2′-methylbenzoyl,[26] semicarbazone[27]) hydrazone copper complexes have been found to demonstrate low cytotoxic activity toward normal mouse embryonic fibroblasts cell line (NIH 3T3) ($IC_{50}$ > 200 μM). However, they showed significantly less activity against HeLa cell lines than cisplatin at the same time. Moreover, transition metal complexes with quinoline Schiff base ligands have kindled many researchers' interest in continuing the subject of many studies, especially as anticancer chemotherapeutic agents.[21, 28] And in previous studies we found that the Cu(II) quinolin hydrazone Schiff base complex showed high anticancer activity against HeLa and other cancer cell lines.[29, 30] Although these quinoline Schiff base copper complexes exhibit good biological activities, their cytotoxicity to normal cell lines is still unsatisfactory which may restrict their application. So it is very interesting to design and synthesize some novel quinoline Schiff base copper complexes with high efficacy and less toxicity.

Taking the significance mentioned above into consideration, we designed and synthesized three copper(II) complexes[Cu(L1)$(NO_3)_2$] (**C1**), [Cu(L2)$Cl_2$] (**C2**) and [Cu(L2)$SO_4]_2{\cdot}H_2O$ (**C3**) with quinoline derived Schiff base ligands (L1=(E)-methyl 4-((quinolin-8-ylmethylene) amino) benzoate, L2=(E)-ethyl 4-((quinolin-8-ylmethylene) amino) benzoate). The interactions of these complexes with HSA/DNA were evaluated through spectrum and molecular docking method. The antiproliferative activities of ligands and **C1**-**C3** in the cell lines were investigated, and the anticancer mechanisms were further surveyed.

## 2. Experimental section

Antibody, CT-DNA, HSA, quinoline-8-carboxaldehyde, benzocaine and 4-amino-benzoic acid methyl ester were purchased from Sigma Chemical Co. (USA). Hep-G2, NCI-H460, MGC80-3, HeLa cell lines and normal liver cells (HL-7702) were obtained from ATCC.

Flow cytometric analysis was carried out using a FACS Aria II flow cytometer**.** Fluorescence spectra were measured on PE LS55 spectrometer. UV-Vis spectra were detected using an Aglient Carry 100. $^1$H NMR spectra were got on Bruker Avance 500 spectrometer. High-resolution mass spectra were recorded on a Thermofisher Scientific Exactive LC-MS mass spectrometer.

### 2.1 Synthesis and structures of Cu(II) complexes

#### 2.1.1 Synthesis

Synthesis of L1 and L2. L1 and L2 ligand were synthesized according to the available methods.[31, 32] In brief, a mixture of quinoline-8-carbaldehyde (1.57 g, 10 mmol) and 4-amino-benzoic acid methyl ester (1.51 g, 10 mmol,) or benzocaine (1.65 g, 10 mmol) in 50 mL methanol was stirred overnight (60 °C). And then the resulting yellow solid products suitable for structural analysis were obtained.

L1. Yield: 93%. Anal. Calcd for $C_{18}H_{14}N_2O_2$: C, H and N of 74.47, 4.86 and 9.65, respectively. Found: C, H and N of 74.35, 4.90 and 9.51, respectively. FT-IR (KBr, $cm^{-1}$): 1704, 1599, 1578, 1274, 1105, 779, 706 and 652. HRMS (ESI): m/z=291.1127 $[M+H]^+$, and calcd for: 291.1134 $[M+H^+]^+$. $^1$H NMR (500 MHz, DMSO-$d_6$) δ 9.84 (s, 1H, -CH=N), 9.05 (d, *J*=3.8 Hz, 1H, ArH), 8.55 (d, *J*=7.2 Hz, 1H, ArH), 8.51 (d, *J*=8.2 Hz, 1H, ArH), 8.24 (d, *J*=8.0 Hz, 1H, ArH), 8.04 (d, *J*=8.2 Hz, 2H, ArH), 7.79 (t, *J*=7.7 Hz, 1H, ArH), 7.67 (dd, *J*=8.3, 4.1 Hz, 1H, ArH), 7.41 (d, *J*=8.3 Hz, 2H, ArH), 3.87 (s, 3H, $CH_3O$).

L2. Yield: 94%. Anal. Calcd for $C_{19}H_{16}N_2O_2$: C, H and N of 74.73, 5. 61 and 9.17, respectively. Found: C, H and N of 74.80, 5.72 and 9.01, respectively. FT-IR (KBr, $cm^{-1}$): 1704, 1599, 1578, 1274, 1105, 779, 706 and 652. HRMS (ESI): m/z=305.1280 $[M+H]^+$, and calcd for: 305.1290 $[M+H^+]^+$. $^1$H NMR (500 MHz, DMSO-$d_6$) δ 9.85 (s, 1H, -CH=N-), 9.05 (dd, *J*=4.1, 1.8 Hz, 1H, ArH), 8.57 (dd, *J*=7.3, 1.2 Hz, 1H, ArH), 8.52 (dd, *J*=8.4, 1.7 Hz, 1H, ArH), 8.26 (dd, *J*=8.1, 1.2 Hz, 1H, ArH), 8.07-8.03 (m, 2H, ArH), 7.81 (t, *J*=7.7 Hz, 1H, ArH), 7.68 (dd, *J*=8.3, 4.2 Hz, 1H, ArH), 7.44-7.39 (m, 2H, ArH), 4.34 (q, *J*=7.1 Hz, 2H,-C<u>H</u>$_2$CH$_3$), 1.35 (t, *J*=7.1 Hz, 3H, -CH$_2$C<u>H</u>$_3$).

Synthesis of **C1, C2** and **C3**. Copper salt (0.15 mmol, $Cu(NO_3)_2{\cdot}3H_2O$ (36.3 mg) for **C1**, $CuCl_2{\cdot}2H_2O$ (25.5 mg) for **C2** and $CuSO_4{\cdot}5H_2O$ (37.5 mg) for **C3**) and ligand (0.15 mmol, L1 for **C1**, L2 for **C2** and **C3**) were put in a thick Pyrex tube, and then the Pyrex tube was quenched in liquid $N_2$ and sealed. They were heated for four days at 80 °C, and programmed cooling to room temperature (5 °C/h). Crystals suitable for X-ray structure analysis were obtained.

**C1**. Green blocks crystal. Yield: 82%. Anal. Calcd for $C_{18}H_{14}CuN_4O_8$ (477.87): C, H and N of 45.24, 2.95 and 11.72, respectively. Found: C, H and N of 45.05, 3.11 and 11.42, respectively. FT-IR (KBr, $cm^{-1}$): 3440, 1704, 1637, 1589, 1409, 1378, 1285, 1184, 1116, 1015, 775, 705, 610, 521, 479 and 430. HRMS (ESI): $C_{18}H_{14}CuN_3O_5$ $[M-NO_3]^+$, calcd for: 415.0230, found 415.0227.

**C2**. Green blocks crystals. Yield: 80%. Anal. Calcd for $C_{19}H_{16}N_2O_2CuCl_2$ (403.34): C, H and N of 52.01, 3.68 and 6.38, respectively. Found: C, H and N of 51.87, 3.55 and 6.59, respectively. FT-IR (KBr, $cm^{-1}$): 3444, 1715, 1595,

View Article Online
DOI: 10.1039/C8MD00223A




1511, 1279, 1184, 1100, 1022, 843, 775, 695, 606, 521, 479 and 433. HRMS (ESI): $C_{19}H_{16}N_2O_2CuCl$ $[M\text{-}Cl]^+$, calcd for: 402.0196, found 402.0183.

**C3**. Bright green blocks crystals. Yield: 78%. Anal. Calcd for $C_{38}H_{32}N_4O_{14}Cu_2S_2$ (959.88): C, H and N of 47.55, 3.36 and 5.84, respectively. Found: C, H and N of 47.15, 3.81 and N 5.65, respectively. FT-IR (KBr, $cm^{-1}$): 3440, 1715, 1637, 1384, 1274, 1142, 838, 780, 659, 574, 490 and 427. HRMS (ESI): $C_{19}H_{17}N_2O_6CuS$ $[M\text{-}H_2O+H]^-$, calcd for: 464.0103, found 464.0048.

### 2.1.2 X-Ray crystallography

The crystal structure data of complexes **C1**-**C3** were collected using a SuperNova CCD Area Detector (Mo-Ka, $\lambda$=0.71073 Å). Data collection and refinement were made using Apex2 software.[33] SADABS program was used for absorption corrections.[34] The structures of complexes **C1**-**C3** were solved through SHELX-97 programs. The complexes **C1**-**C3** crystallographic information is given in Table S1 and Table S2.

## 2.2. HSA binding studies

Fluorescence method. A 2.0 mL HSA aqueous solution (1 μM) was titrated by the **C1**-**C3** and L1, L2. The changes of fluorescence of HSA were recorded at excitation wavelength =275 nm. By using the Scatchard equation (Eq. (1)):[35] $\log[(F_0 - F)/F]=\log K_{bin}+n\times\log(Q)$, the binding constant ($K_{bin}$) of test compounds to HSA were analyzed. Furthermore, the quenching rate constant ($K_q$) and quenching constant ($K_{sv}$) can be calculated as (Eq. (2)): $F_0/F=1+K_q\tau_0[Q]=1+K_{sv}[Q]$.Where $F_0$ is fluorescence of HSA; $F$ is the fluorescence of HSA after adding test compound; [Q] is the test compound concentration; $\tau_0$ =4.43 ns.[36] And the synchronous fluorescence spectra of HSA were also scanned when Δλ=60, 15 nm, respectively.

UV-visible absorption method. The concentration of the compound and HSA was kept at 2.5 μM. The absorption spectra are scanned from 250 to 350 nm at room temperature.

## 2.3. DNA binding studies

CT-DNA/EB system (10 μM) was titrated by the test compounds ranging from 0 to 30 μM and their fluorescence spectra were measured. And the quenching constant ($K_q$) and the apparent DNA binding constant ($K_{app}$) were given using the Eq. (3): $I_0/I = 1+K_q[Q]$ and Eq. (4): $K_{EB}$ [EB] = $K_{app}$ [complex], [37, 38] respectively. Where $I_0$ is the fluorescence of CT-DNA/EB system. And $I$ is the fluorescence of CT-DNA/EB after adding test compounds. [Q] is the compound concentration; $K_{EB}$ = $1.0\times10^7$ $M^{-1}$; [complex] is the compound concentration at 50 % fluorescence of CT-DNA/EB system.

## 2.4. Molecular docking analysis

Docking studies were performed in order to analyze interactions of test complex to HSA /DNA. The AutoDock Tools with 1.5.6 docking programmers and Autodock Vina were employed to analyze the molecular docking.[39, 40] The HSA and B-DNA crystal structures were got from the bank of Protein Data (HSA: PDB ID: 1E7H; DNA: PDB ID: 1BNA; $(CGCGAATTCGCG)_2$). The structure of complex and HSA/DNA was prepared according to reference method.[41, 42] Briefly, the Cu(II) complexes structures were converted into PDB format from cif format using Mercury software. The structure of DNA and protein was modified to include polar hydrogen atoms and water molecules and the ligands were removed, and Gasteiger charges were added to the complex by Autodock Tools (ADT) before performing docking calculations.

## 2.5. MTT assays

The cytotoxic of all compounds against cell lines was screened through MTT standard method. In brief, in a 96-well plate, the cells were seeded ($5\times10^3$cells/well) and cultured for 24 h in 5% $CO_2$. And test compounds (0-100 μM) were added and further incubated for 48 h. In the each well, 10 μL, 5 mg/mL MTT solution was put into and cultured for 5 h, and then DMSO (100 μL) was injected after removal of the supernatant. Finally, we used the ELISA microplate reader to measure the absorbance of each well and calculate the $IC_{50}$ values.

## 2.6. Cell cycle distribution analysis and cellular uptake

After HeLa cells were cultured, the **C3** was added at indicated concentration. The mixture was kept in 5 % $CO_2$ at 37 °C for 24 h. And then, we collected and fixed the cells with ice-cold ethanol (70 %, -20 °C) overnight. The 100 μg/ml Rnase A was put into the cells and further cultured (30 min, 37 °C). In the dark, the cells were stained using PI for 15 min. Finally, the above solution was tested and analyzed immediately.

HeLa cell was treated with **C3** (10 μM) and cultured for 24 h. The cells were washed five times with ice-cold buffer and treated with concentrated $HNO_3$. The amount of Cu(II) compound in cells was monitored by ICP-MS.

## 2.7. Cells apoptosis

HeLa cells were cultured with **C3** at different concentrations for 48 h, and then harvested and suspended in buffer of annexin-binding (200 μL 1×). We used the annexin V (5 μL) and PI (5 μL) to stain the cell suspension in the dark (15 min). And binding buffer (300 μL 1×) was follow put into the while gently mixing.

View Article Online
DOI: 10.1039/C8MD00223A




Finally, the mixtures were measured immediately using FACS Calibur flow cytometer (BD).

## 2.8. ROS level

The HeLa cells were treated with **C3** (0-20 μM) and incubated in $CO_2$ incubator (24 h, 37 °C) after attachment. HeLa cells were then collected and incubated for 30 min at 37 ºC with $H_2$DCFDA (10 μM) in serum-free medium. Afterward, HeLa cells were washed and then the fluorescence intensity was recorded.

## 2.9. Mitochondrial membrane potential

After HeLa cells were seeded and incubated with complete DMEM for 24 h, the **C3** was added and further cultured (24 h). The cells were collected and re-suspended in PBS buffer contains pre-warmed JC-1 (5 μg/mL) and kept incubation at 37 °C (30 min). Subsequently, we used PBS buffer to wash the cells three times. Finally, the mixture was measured immediately by FACS Calibur flow cytometer (BD).

## 2.10. Western blot assay

Briefly, after the HeLa cells were cultured overnight, **C3** was added and further incubated (24 h). The total proteins were extracted after cell-lysing. And the extract was loaded onto SDS polyacrylamide gel, and follow transferred to PVDF membranes. 5 % BSA in TBST buffer was used to block the membrane. The primary antibodies were added and incubated overnight (4 °C). After washing, the secondary antibody was also added and cultured (120 min). Finally, the signal of immuno reactive was detected.

# 3. Results and Discussion

## 3.1. Characterization of L1, L2, **C1**-**C3**

L1, L2, **C1**-**C3** were synthesized and characterized via the above synthetic method (Fig.S1-S12). The characterization results indicated that the structure of these compounds is consistent with the compositions.

The crystal structures of **C1** and **C2** are shown in Fig.1. The **C1** and **C2** belong to the triclinic (*P*-1) and monoclinic ($P2_1/n$) crystal system, respectively. In complex **C1**, the copper atom is four-coordinate, bonded to two N (N1 and N2) donors from L1 ligand and two terminals $NO_3^-$. All Cu-X bond lengths are in good consistent with previously literature of Cu(II) complex.[43] In complex **C2**, copper atoms are four coordinated by two nitrogen atoms (N1 and N2) of L2 ligand and two terminal chlorine (Cl1 and Cl2).

Compared to **C1** and **C2**, the **C3** is a dinuclear neutral complex, $[Cu(L2)SO_4]_2$, with $SO_4^{2-}$ anion bridges (Fig. 1). Every central copper(II) in the dimer is five-coordinated in the form of a slightly distorted square pyramidal geometry with the τ=0.01.41 Interestingly, the Cu-N(quinolin) lengths (Cu1-N1 = 1.985 (4) Å in C1, Cu1-N1 = 1.987 (2) Å in **C2** and Cu1-N2 = 1.979 (5) Å in **C3**) of complexes **C1**-**C3** are longer than the Cu-N(imine) lengths (Cu1-N2=1.972 (4) Å in C1, Cu1-N2 = 1.9855 (19) in **C2** and Cu1-N1=1.958 (5) Å in **C3**) of these complexes, respectively, which is possibly due to weaker π-back-bonding in the Cu-N (quinolin) bond than in the Cu-N (imine) bond.

## 3.2. Stability of **C1**-**C3**

The metal complexes stability has an effect on their antitumor activity. Therefore, the hydrolytic stabilities of the Cu(II) complexes were investigated. The UV-Vis absorption spectra of **C1**-**C3** in aqueous solutions (TBS, pH 7.4, 1 % DMSO) at different times (0, 24 and 48 h) are shown in Fig. S13. The UV-Vis spectra do not differ significantly from those observed even after 48 h at laboratory temperature, which indicated that the **C1**-**C3**

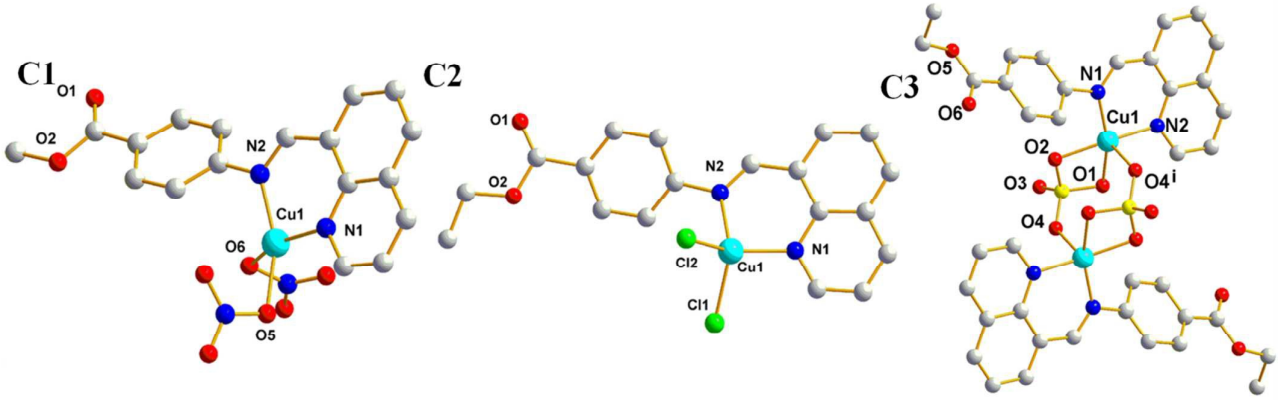


Fig. 1. ORTEP drawing of the complex **C1**-**C3** with atom numbering scheme. Color scheme: Cu, aqua; O, red; N, blue; C, gray; Cl, green.

View Article Online
DOI: 10.1039/C8MD00223A




were stable in TBS buffer within 48 h.

## 3.3 HSA binging ability

The binding ability of anticancer agents with HSA affects their distribution, uptake, transfer, metabolism and mechanism of action to cancer cells.[44-46] First, we studied the nature of the **C1**-**C3** binding with HSA using fluorescence and UV-Vis absorption method.

The fluorescence spectral changes were investigated before and after titration using the Cu(II) complexes (Fig. 2-A, B, C) and ligands (Fig. S14). Addition of these compounds to HSA resulted in essential fluorescence quenching of HSA with small blue shift (59 %, 1 nm, **C1**; 60 %, 3 nm, **C2**; 62 %, 7 nm, **C3**; 43 %, 1 nm, L1; 47 %, 2 nm, L2). And the quenching efficiency of these complexes for HSA was more than free ligands. These facts indicated that the binding of the test compounds to HSA did happen and the binding sites of HSA are buried in a hydrophobic environment.

To further study the quenching process, the $K_q$, $K_{sv}$ and $K_{bin}$ were assessed using the Eq(1) and Eq(2) (Fig. S15) (Table 1). As can be seen from Table 1, the higher $K_{sv}$ and $K_{bin}$ values of **C3** than the **C1** and **C2** may be due to its higher solubility in aqueous medium. The $K_q$ values of these complexes are 1000-fold higher than the maximum collisional quenching constant ($2.0\times10^{10}$ mol $L^{-1}$ $s^{-1}$).[34] So the fluorescence of HSA are quenched by these Cu(II) complexes through static quenching processes. And these larger values of $K_{sv}$ and $K_{bin}$ demonstrated strong interaction of **C1**-**C3** with HSA.

UV-vis absorption spectroscopy is a simple method to explore the type of quenching mechanism of HSA. So, we chose **C3** as an example for further study of the quenching mechanism. The absorption intensity of HSA at 280 nm was enhanced and a slight blue shift of about 2 nm was observed with the addition of **C3** (Fig. S16), which demonstrated that the quenching of the test compounds to the fluorescence of HSA is mainly via static processes.

Furthermore, synchronous fluorescence spectra were used for the analysis of changes in microenvironment around the fluorophore functional groups. The information about microenvironment for tryptophan and tyrosine was reflected when Δλ=60 nm and 15 nm, respectively.[47, 48] Synchronous fluorescence spectra of HSA were obtained with different concentration of the **C1**-**C3** (Fig. S17). The addition of test compounds gradually leads to hypochromic effect of HSA. Moreover, when Δλ=60 nm, the maxima emission wavelength of HSA not only decreased gradually but also accompanied by a slight blue shift (1 nm for **C1** and **C2**, 2 nm for **C3**). However, the maximum emission wavelength has no shift at Δλ=15 nm. The results demonstrated that the **C1**-**C3** bind effectively with HSA, and thus quench the fluorescence of tyrosine and tryptophan residues of HSA. And the fluorescence changes also indicate that the interaction of them may occur in domain II because the Tyr and Trp residues are located in domain II of HSA.[42,49] These observed changes of fluorescence are different from the results obtained for cisplatin which induce the emission wavelength of HSA red-shifted and it bound to HSA mainly via covalent bonds.[49,50,51] Therefore, the results suggest that the interaction of **C1**-**C3** with HSA should be noncovalent and reversible.[49]

Table 1. Stern-Volmer quenching constants and binding parameters of the HSA-complexes drug system at 295 K.

| | $K_q$ ($M^{-1}$ $s^{-1}$) | $K_{sv}$ ($M^{-1}$) | $K_{bin}$ ($M^{-1}$) | n |
|---|---|---|---|---|
| **C1** | $6.36\pm0.31\times10^{13}$ | $2.83\pm0.14\times10^{5}$ | $0.94\pm0.09\times10^{8}$ | 1.37 |
| **C2** | $6.49\pm0.25\times10^{13}$ | $2.89\pm0.11\times10^{5}$ | $1.15\pm0.04\times10^{8}$ | 1.49 |
| **C3** | $7.42\pm0.27\times10^{13}$ | $3.30\pm0.12\times10^{5}$ | $1.60\pm0.07\times10^{8}$ | 1.51 |
| L1 | $3.12\pm0.18\times10^{13}$ | $1.38\pm0.08\times10^{5}$ | $0.47\pm0.05\times10^{6}$ | 1.29 |
| L2 | $4.02\pm0.20\times10^{13}$ | $1.78\pm0.09\times10^{5}$ | $1.20\pm0.09\times10^{6}$ | 1.38 |

The high-performance liquid chromatographic (HPLC)[52] was often used to study the interaction mode of guest molecules and HSA. The feature of chromatographic spectrum of mixture of **C3** or L2 and HSA are similar to the pure HSA, indicating that binding of **C3** and L2 induces slight structural changes in the protein (Fig. S18). These experiment results imply that the nature of the interaction of **C1**-**C3** and their respective ligands with HSA is proposed to be noncovalent.[42, 52]

The above results confirmed that the **C1**-**C3** exhibit prominent HSA binding ability via noncovalent interactions. And the binding ability of these complexes for HSA was more than free ligands. Meanwhile, these complexes simultaneously weakened the fluorescence of tyrosine and tryptophan, but their interaction affected the micro-region of tryptophan more than the tyrosine. The strong binding ability of the complexes to HSA suggested that the **C1**-**C3** can be stored in protein easily, then be carried to the objective area and be released from the protein to the desired targets.[29]

## 3.4. DNA Binding

DNA is one of the main molecular targets for cancer therapeutics.[53, 54] Hence, the fluorescence method based on the EB competitive experiment is used to investigate the nature of the interaction of **C1**-**C3** (Fig.2-D, E,F) and ligand (Fig.S19) with CT-DNA. The emission band of CT-DNA/EB was gradually decreased when these compounds was titrated. And the effect of hypochromism of complex to CT-DNA/EB system is more than corresponding ligand. Furthermore, the $K_q$ and $K_{app}$ values are analyzed (Table 2) according to the Eq (3) and (4) (Fig. S20) for evaluating the binding ability of complexes and free ligand. As can be seen from the Table 2, the binding of **C1**-**C3** with CT-DNA is stronger than that of the free ligand. The higher DNA binding

View Article Online
DOI: 10.1039/C8MD00223A


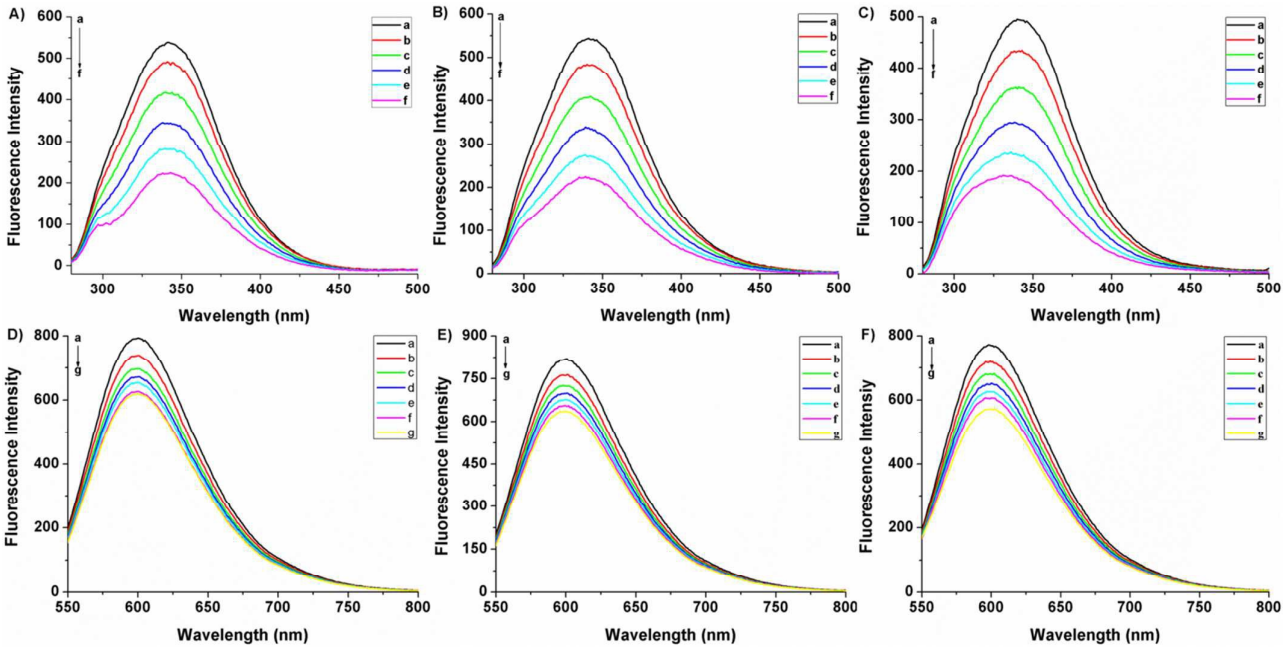


Fig. 2. The emission spectrum of HSA (1μM; λex=280 nm) in the absence and presence of **C1** (A), **C2** (B) and **C3** (C) with increasing concentrations (0, 1.0, 2.0, 3.0, 4.0 and 5.0 μM). And fluorescence quenching spectra of DNA-EB (10 μM) in the presence of **C1** (D), **C2** (E) and **C3** (F) (0, 5.0, 10, 15, 20, 25 and 30 μM).

affinity of **C3** may be due to its solubility in aqueous medium.[55]

The complexes have no UV-vis absorption (Fig. S13) and fluorescence excitation spectra in 550-700 nm range (Fig. S21), which indicated that these compounds cannot quench the fluorescence of EB through using the inner effect or energy transfer mechanism. It may be inferred that the EB is being replaced efficiently from the binding sites of CT-DNA by these test compounds. The above results demonstrated that the **C1**-**C3** can interact with CT-DNA via an intercalative mode and their binding ability is greater than the free ligand.[56]

## 3.5 Molecular docking studies

Docking studies were investigated in order to provide complement of the spectroscopic results and more insight into complex-HSA interaction. The resulting docked pattern of **C3** with the lowest energy and the entire protein structure is respectively shown in Fig.3 and Fig. S22. The results reveal that the complex **C3** bound at hydrophobic cavities of HSA subdomains IIIA and IIA, but mainly in IIA. And it was surrounded by Lys199, Ser202, Phe211, Ala210, Trp214, Val344, Leu453, Leu457, Leu481, Arg485, Ser454, Glu450 and Ser342. Molecular models show that complexes **C2** (Fig. S23-B) and **C3** are almost in the same position. The docking results showed potential Trp214. **C1** (Fig. S23-A) is located in subdomain IIA hydrophobic cavity, and it is surrounded by Leu260, Leu219, Leu238, Lys199, Arg218, Arg257, His242, Val241, π-π stacking interactions of **C2** and **C3** with the residue Ala291, Glu153, Gln196, Ser192, His288 and Ser287. The methyl 4-aminobenzoate fragment of the **C1** interacts with Gln196 and Glu153 amino acid residues by hydrogen bonds. The lipophilic quinoline fragment of the **C1** is coiled into a hydophobic

Table 2. Stern-Volmer constant (*Kq*) and the apparent binding constant (Kapp) for the Cu(II) complexes.

| | $K_q$ ($M^{-1}$ $s^{-1}$) | $K_{app}$ ($M^{-1}$) |
|---|---|---|
| **C1** | 0.93±0.04×10$^4$ | 0.95±0.05×10$^4$ |
| **C2** | 0.92±0.05×10$^4$ | 0.94±0.06×10$^4$ |
| **C3** | 1.10±0.06×10$^4$ | 1.11±0.06×10$^4$ |
| L1 | 0.22±0.02×10$^4$ | 0.23±0.02×10$^4$ |
| L2 | 0.44±0.03×10$^4$ | 0.45±0.02×10$^4$ |

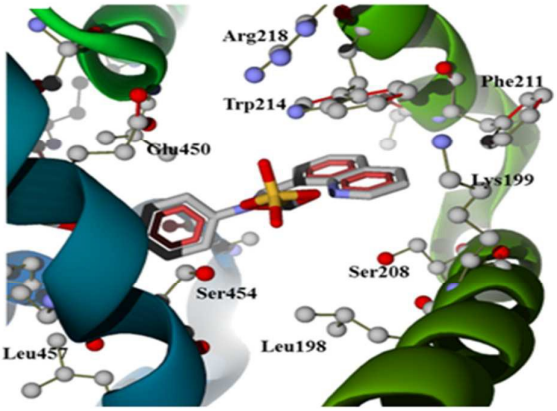


Fig. 3. Molecular docked structure of the C3 interacting with HSA (PDB ID: 1E7H).

View Article Online
DOI: 10.1039/C8MD00223A




channel lined by Leu260, Leu219, Leu238, Ala291 and Val241. We can fount that their binding sites with HSA are different from cisplatin.[57] The lowest binding energies of **C1**, **C2**, and **C3** respectively are -9.3, -10.8, and -11.8 kcal $mol^{-1}$, which suggested that their bindingaffinity ability with HSA is more than the other copper(II) complex.[58]

The interaction of **C1**-**C3** with B-DNA (PDB ID: 1BNA) were also studied by docking studies. Energetically favourable docked poses obtained from the molecular docking of the **C3** to the B-DNA is shown in Fig. 4, and the **C1**, **C2** is demonstrated in Fig. S24. And their lowest binding energies are -8.1 (**C1**), -8.0 (**C2**), and -8.4 (**C3**) kcal $mol^{-1}$, respectively, and those are lower than that for the other copper(II) Schiff base complexes.[59] Meanwhile, the **C1**-**C3** fitted well into the curved contour of the B-DNA target into the minor groove region, which brings about hydrogen bonds, hydrophobic interactions and van der Waals with DNA functional groups that define the groove. And their interaction region with DNA is different from the cisplatin which binding to the DNA major groove faces inward.[60] Furthermore, the energy minimized structures suggest that the **C1**-**C3** stabilized by π-π stacking (edge to face interactions). Therefore, these data suggested that the docking studies results corroborated well with spectroscopic results.

## 3.6. $IC_{50}$ level

The ligand, metal salt, **C1**-**C3** and cisplatin cytotoxicities of in vitro toward the tested cells were examined via MTT method. And the $IC_{50}$ values obtained are summarized in Table 3.

The **C1**-**C3** showed a potent inhibition activity toward Hela, with $IC_{50}$ in the micromolar range and obviously lower than cisplatin. In contrast, the free ligand, and metal salt displayed relatively low activity toward HeLa cells. The enhanced antiproliferative activity of **C1**-**C3** may result from the synergistic effect of Cu(II) ion and ligand. Despite this potency, the Cu(II) complexes were much less toxic toward human normal cell (HI-7702), with $IC_{50}$ values ranging from 60.39 to 92.81 μM, which are significantly higher than that of cisplatin (23.02 μM). And the cytotoxicity of **C1**-**C3** on the normal HL-7702 cells respectively was 4.7, 5.9 and 6.1 times lower than the activity on HeLa cells, which suggested that the **C1**-**C3** might selectively inhibition activity against HeLa cell.

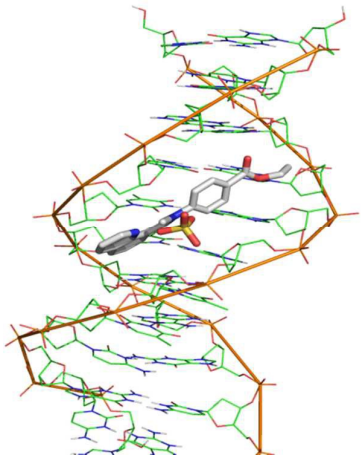

Fig. 4. Molecular docked model of complex **C3** with DNA (PDB ID: 1BNA).

Table 3. $IC_{50}$[a] (μM) values of L1, L2 and **C1**-**C3** on the selected cells for 48 h.

| Compound | Hep-G2 | NCI-H460 | MGC80-3 | HeLa | HL-7702 |
|---|---|---|---|---|---|
| 4-amino-benzoic acid methyl ester | >100 | >100 | >100 | >100 | >100 |
| Benzocaine | >100 | >100 | >100 | >100 | >100 |
| L1 | >100 | >100 | >100 | >100 | >100 |
| L2 | >100 | >100 | >100 | >100 | >100 |
| **C1** | >100 | >100 | >100 | 18.72 ± 1.03 | 87.70 ± 4.01 |
| **C2** | >100 | 35.45± 2.35 | 16.87 ± 2.01 | 15.76± 1.19 | 92.81± 6.03 |
| **C3** | >100 | >100 | 17.52± 1.81 | 9.98± 0.87 | 60.39± 5.86 |
| Cisplatin | 27.31± 2.01 | 47.68± 1.98 | 21.28± 2.81 | 35.25± 2.80 | 23.02± 5.68 |
| Copper(II) salt | >100 | >100 | >100 | >100 | >100 |

In comparison, the cytotoxic activity toward HeLa cell follows the order **C3**>**C2**>**C1**, which is consistent with DNA/HSA binding results. These results implied that the introduction of the drug molecule of benzocaine was more effective for enhancing the anticancer activity than that of 4-amino-benzoic acid methyl ester.

Moreover, the $IC_{50}$ values of these complexes, especially **C3** to HeLa cell are comparable or lower than most of the previously reported quinoline derived Schiff base complexes.[20, 21, 23-30] Meanwhile, the cytotoxic activity toward HL-7702 was clearly decreased comparing with our previously reported quinoline-8-carboxaldehyde hydrazone copper complexes,[29, 30] which may be that introduction of the benzocaine into quinoline scaffolds induces a synergistic cytotoxicity. Hence, the results suggested that the Cu(II) complexes possess well selectivity between normal and cancer cells, and thus show application potential in human cervical cancer chemotherapy.

Base on the above results, it can be inferred that **C3** possesses higher cytotoxicity toward HeLa cell lines compared to the free ligand as well as **C1** and **C2**. Thus, **C3** was selected to investigate the anticancer mechanism.

## 3.7. Possible anticancer mechanism of **C3**

Because complex **C3** exhibits the highest cytotoxicity to HeLa, the complex was used for further cellular studies to understand its mechanism of action. Most previously reported cell apoptosis induction and cell cycle arrest closely correlated to cancer cells death,[61, 62] we therefore monitored features related to these pathways.

View Article Online
DOI: 10.1039/C8MD00223A




The cellular uptake properties affect metal-based anticancer drug antiproliferative performance, so we first assessed the uptake of **C3** in HeLa cells using ICP-MS assay. The accumulated amount of **C3** was 9.6±2.5 nM/$10^6$ cells in the HeLa cells after 24 h of treatment. Subsequently, the cell cycle in HeLa cells induced by **C3** (5, 10 and 20 μM) was examined by flow cytometry (Fig. 5). With the increase of the complex **C3**, the S-phase and G2/M-phase cells population reduced gradually. However, a dramatically increase in G0/G1-phase was obtained from 53.79 % to 83.66 %. The results indicated that **C3** stalled the cell cycle at the G0/G1-phase in a concentration-dependent manner. It is known that cyclin-dependent kinases (CDKs) and cyclins complexes affect the cell cycle progression at each phase.[63] Therefore, the expression of cell cycle regulatory proteins of G0/G1-phase was determined using western blotting assay to study the molecular mechanisms of the complex **C3** induced G0/G1-phase block (Fig. 6). As can be seen from Fig. 6, the progression of CDK2, cyclin D1 and E reduced in a dose-dependent manner. And the expression of CDK4 has almost no changes. The observed phenomenon revealed that inhibition of the activity of G0/G1-phase-promoting cyclin-Cdk complexes by limiting the supply of CDK2, cyclins D1 and E1 may be a mechanism by which the C3 mediated growth G0/G1-phase arrest.

It has been reported that most metal anticancer agents generally kill tumor cells through induction of apoptosis,[64, 65] we therefore monitored the ability of complex **C3** to promote apoptosis in HeLa cells (Fig. 7). It was found that the populations of the apoptotic HeLa cells (both at the early stage and the late stage of apoptosis, Q2+Q3) distinctly increased in a dose-dependent manner when incubating with the **C3**. And the apoptosis populations of HeLa cells in early-and late-stage were 16.7% and 9.28%, respectively, which

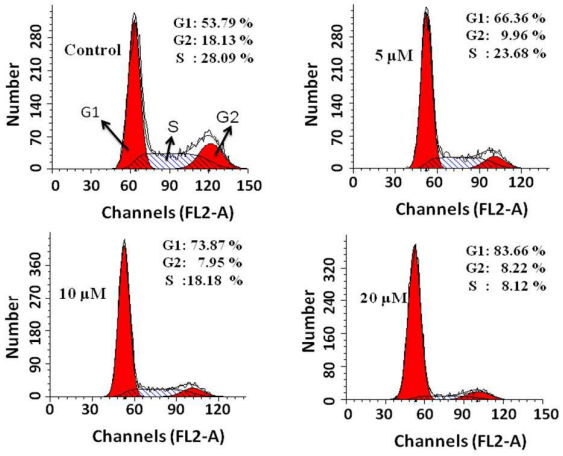


Fig. 5. Cell cycle analysis by flow cytometry for HeLa cells treated by **C3** (5, 10 and 20 μM

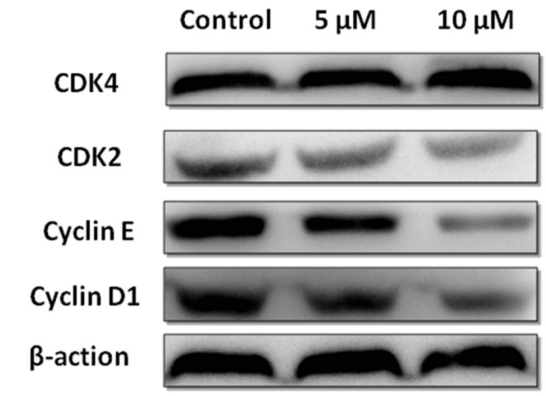


Fig. 6. Western blot was used to determine the expression of CDK2, CDK4, cyclin E, cyclin D1 in HeLa cells treated with C3 (5 and 10 μM).

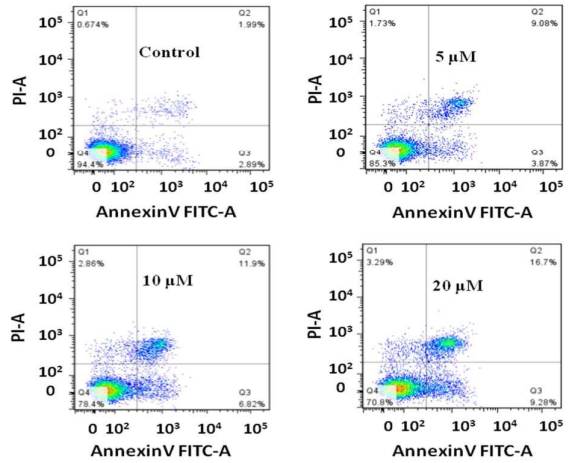


Fig. 7. Annexin-V/propidium iodide assay of HeLa cells treated by **C3** (5, 10 and 20 μM) measured by flow cytometry.

suggested that cell apoptosis in HeLa cells can be effectively induced by complexes.

Mitochondrial dysfunction plays an importance in triggering various apoptotic pathways.[66] To confirm whether mitochondrial dysfunction induces cells apoptosis, we used flow cytometry to measure the mitochondrial membrane potential (MMP) (Fig. 8). The **C3** led to reduce in MMP compared with the control cells, and exhibited in a dose-dependent manner, which implies that the mitochondrially-mediated apoptosis was activated.

In apoptosis pathway, reactive oxygen species (ROS) elevation closely associated with mitochondrial dysfunction.[67] Thus, the complex **C3** catalytic ability of the intracellular ROS elevation in HeLa cells was monitored by flow cytometry and the fluorescent 2',7'-dichlorofluorescein (DCF) probe. As shown in Fig. 9A, comparing with the control groups, incubation of HeLa cells with the complex **C3** can increase the levels of DCF fluorescence and lead to the red shift of the fluorescence

View Article Online
DOI: 10.1039/C8MD00223A




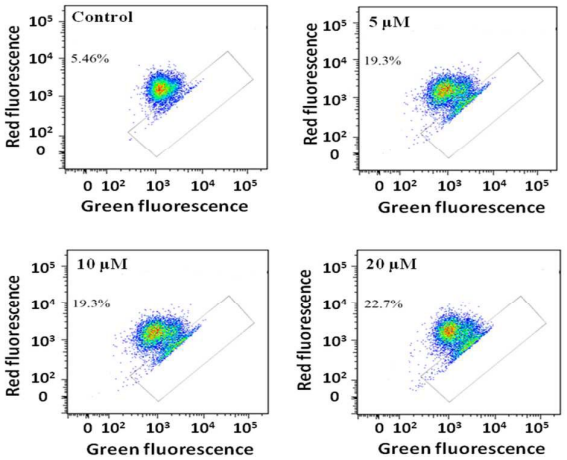


Fig. 8. Effects of **C3** (5, 10 and 20 μM) on MMP analyzed by JC-1 staining and flow cytometry.

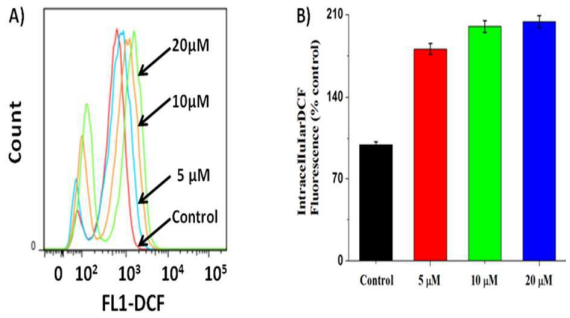


Fig. 9. A) Analysis of ROS levels by flow cytometry after HeLa cells were treated with vehicle, **C3** at indicated concentrations for 12 h and stained with H2DCFDA. B) Quantification of the flow cytometric results in (A) showing the percentage of cells with increased intracellular DCF oxidation compared to control cells. Results are the mean ±SD (n=5): (**) p<0.01.

peak, which infers that the **C3** increased oxidative damage to the HeLa cell. The level of ROS shows a dose-dependent manner (Fig. 9B).

The Bcl-2 family proteins have been verified as key regulators of apoptosis.[68] To further study the mechanism of cells apoptosis, we tested the Bcl-2 family proteins expression through **C3** treated with cells (Fig. 10).

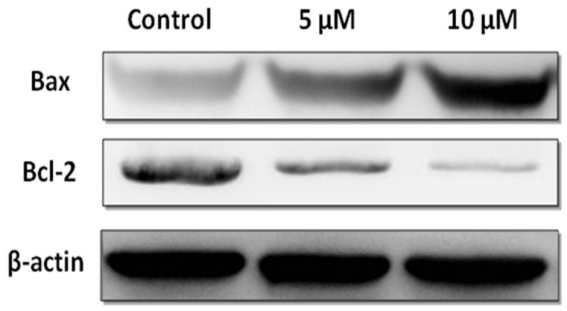


Fig. 10. Western blot was used to determine the expression of Bcl-2 and Bax in HeLa cells treated with **C3** (5 and 10 μM).

The western blot data reveal that the complex induced expression significantly down-regulation of Bcl-2 protein and slightly up-regulation of Bax protein in a concentration-dependent manner. These results demonstrated that **C3** could activate the Bcl-2 and Bax proteins and decrease the ratio of Bcl-2 protein to Bax protein, which lead to the mitochondrial release of apoptogenic factors in HeLa cells and ultimately induced cells apoptosis.

## 4. Conclusions

In conclusion, three Cu(II) complexes of quinoline derived Schiff base were designed, synthesized and characterized. The **C1**-**C3** display high quenching ability of HSA fluorescence and strong binding activity by noncovalent interactions, and hydrophobic interaction with HSA through sub domain IIA and IIIA cavity. Moreover, the complexes effectively bind to DNA by intercalative mode, and they fit well into the curved contour of the DNA target into the minor groove region. Cytotoxicity assay reveal that these complexes enhanced significantly the cytotoxic activity toward HeLa cell lines with their IC50 values being markedly lower than those of cisplatin, the ligands and metal salt. The *in vito* antiproliferative activities of **C2** and **C3** against the HeLa cell are greater than that of **C1**, suggesting that the introduction of the drug molecule of benzocaine was more effective for enhancing the anticancer activity than that of 4-amino-benzoic acid methyl ester. Meanwhile, the complexes show low cytotoxic against normal HL-7702 cell lines, which demonstrate that these complexes have more selective for HeLa cell than for normal HL-7702 cells. The mechanism studies indicate that **C3** can regulate the expression of CDKs along with cyclins, and arrest cell cycle at the G0/G1 phase. At the same time, the **C3** can effectively induce HeLa cell lines apoptosis via the ROS-mediated mitochondrial pathways, and activate the Bcl-2 family proteins. In general, the introduction of active medicament into ligand could improve the biologic effects of the copper complexes with quinoline derived Schiff base in the respect of DNA/HSA affinity and cell cytotoxicity. The present work implies that it may be helpful for the design and development of the potential anticancer complex by using the modified clinical drug as ligand.

## Conflicts of interest

The authors declare no competing interests.

## Acknowledgements

This work was support by National Natural Science Foun dation of China (No. 21565007,21271050 and 51572050), Guangxi Natural Science Foundation (No. 2015GXNSFDA

View Article Online
DOI: 10.1039/C8MD00223A


139007), State Key Laboratory Cultivation Base for the Chemistry and Molecular Engineering of Medicinal Resources, Ministry of Science and Technology of China (CMEM2014-A06, CMEMR2012-A08), IRT_16R15, Talent's Small Highland Project of Guangxi Medicine Industry (No. 1509).

## References

1 C. Santini, M. Pellei, V. Gandin, M. Porchia, F. Tisato and C. Marzano, Chem. Rev., 2014, 114, 815-862.
2 A. Gupte and R.J. Mumper, Cancer Treat. Rev., 2009, 35, 32-46.
3 F. Tisato, C. Marzano, M. Porchia, M. Pellei and C. Santini, Med. Res. Rev., 2010, 30, 708-749.
4 L. Ruiz-Azuara and M.E. Bravo-Gomez, Curr. Med. Chem., 2010, 17, 3606-3615.
5 J. Y. Hu, C.L. Liaob R.N. Mao, J.S. Zhang, J.A. Zhao and Z.Z. Gu, Med. Chem. Commun., 2018, 9, 337-343.
6 C. Santini, M. Pellei, V. Gandin, M. Porchia, F. Tisato and C. Marzano, Chem. Rev., 2014, 114, 815-862.
7 I. Kostova and L. Saso, Curr. Med. Chem., 2013, 20, 4609-4632.
8 K. Sztanke, A. Maziarka, A. Osinka and M. Sztanke, Bioorg. Med. Chem., 2013, 21, 3648-3666.
9 P. H. Wang, J. G. Keck, E. J. Lien and M. M. Lai, J. Med. Chem., 1990, 33, 608-614.
10 A. Ganguly, P. Chakraborty, K. Banerjee and S. K. Choudhuri, Eur.J. Pharm. Sci., 2014, 51, 96-109.
11 R. D. Ghosh, P. Chakraborty, K. Banerjee, A. Adhikary, A. Sarkar, M. Chatterjee, T. Das and S. K. Choudhuri, Mol. Cell. Biochem., 2012, 364, 309-320.
12 A. Ganguly, S. Basu, K. Banerjee, P. Chakraborty, A. Sarkar, M. Chatterjee and S. K. Chaudhuri, Mol. BioSyst., 2011, 7, 1701-1712.
13 X.Q. Zhou, Y. Li, D.Y. Zhang, Y. Nie, Z.J. Li, W. Gu, X. Liu, Ji.L. Tian and S.P. Yan, Eur. J. Med. Chem., 2016, 114, 244-256.
14 C.X. Lu, A. Eskandari, P. B. Cressey and K. Suntharalingam, Chem. Eur. J., 2017, 23, 1366-1374.
15 Y.Q. Hu, C. Gao, S. Zhang, L. Xu, Z. Xu, L.S. Feng, X. Wu and F. Zhao, Eur. J. Med. Chem., 2017, 139, 22-47.
16 O. Afzal, S. Kumar, M.R. Haider, M.R. Ali, R. Kumar, M. Jaggi and S. Bawa, Eur. J. Med. Chem., 2015, 97, 871-910.
17 R. Musiol, Expert Opin Drug Discov., 2017, 12, 583-597.
18 N. Srimongkolpithak, S. Sundriyal, F.L. Li, M. Vedadi and M. J. Fuchter, Med. Chem. Commun., 2014,5, 1821-1828.
19 S. Adsule, V. Barve, D. Chen, F. Ahmed, Q.P. Dou, S. Padhye and F.H. Sarkar, J. Med. Chem., 2006, 49, 7242-7246.
20 Saswati, A. Chakraborty, S. P. Dash, A. K. Panda, R. Acharyya, A. Biswas, S.Mukhopadhyay, S. K. Bhutia, A. Crochet, Y. P. Patil, M. Nethajie and R. Dinda, Dalton Trans., 2015, 44, 6140-6157.
21 Y.P. Du, W. Chen, X. Fu, H. Deng and J.G. Deng, RSC Adv., 2016, 6, 109718-109725.
22 T. Thirunavukkarasu, H. A. Sparkes, K. Natarajan and V. G. Gnanasoundari, Inorg Chim Acta., 2018, 473, 255-262.
23 J. Lu, Q. Sun, J.L. Li, L. Jiang, W. Gu, X. Liu, J.L. Tian and S.P. Yan, J. Inorg. Biochem., 2014, 137, 46-56.
24 [23] D. S. Raja, N. S.P. Bhuvanesh and K. Natarajan, Inorg Chim Acta., 2012, 385, 81-93.
25 D. S. Raja, N. S.P. Bhuvanesh and K. Natarajan, Eur. J. Med. Chem., 2012, 47, 73-85.
26 D. S. Raja, E. Ramachandran, N. S.P. Bhuvanesh and K. Natarajan, Eur. J. Med. Chem., 2013, 64, 148-159.
27 D. S. Raja, N. S. P. Bhuvanesh and K. Natarajan, Inorg. Chem., 2011, 50, 12852-12866.
28 T. R. Todorović, J. Vukašinović, G. Portalone, S. Suleiman, N. Gligorijević, S. Bjelogrlić, K. Jovanović, S. Radulović, K. Anđelković, A. Cassar, N. R. Filipović and P. Schembri-Wismayer, Med. Chem. Commun., 2017, 8, 103-111.
29 K. Hu, F.Y. Li, Z. Zhang and F.P. Liang, New J. Chem., 2017, 4, 2062-2072.
30 K. Hu, G.M. Zhou, Z. Zhang, F.Y. Li, J.G. Li and F.P. Liang, RSC Adv., 2016, 6, 36077-36084.
31 B.S. Creaven, B. Duff, D.A. Egan, K. Kavanagh, G. Rosair, V.R. Thangella and M. Walsh, Inorg. Chim. Acta, 2010, 363, 4048-4058.
32 M.-F. Zaltariov, M. Cazacu, M. Avadanei, S. Shova, M. Balan, N. Vornicu, A. Vlad, A. Dobrov and C.-D. Varganici, Polyhedron, 2015, 100, 121-131.
33 E.C.P. APEX2 "*Program for Data Collection and Integration on Area Detectors*" BRUKER AXS Inc., Madison, WI 53711-5373 USA.
34 G.M. Sheldrick, SADABS: *Program for Empirical Absorption Correction of Area Detector Data*, University of Göttingen, Germany, 1996.
35 O.K. Abou-Zied and O.I. Al-Shihi, J. Am. Chem. Soc., 2008, 130, 10793-10801.
36 J.R. Lakowicz and G. Weber, Biochemistry, 1973, 12, 4161-4170.
37 M. Lee, A.L. Rhodes, M.D. Wyatt, S. Forrow and J.A. Hartley, Biochemistry, 1993, 32, 4237-4245.
38 M. V. Lunagariya, K. P. Thakor, R. R. Varma, B. N. Waghela,C. Pathak and M. N. Patel, Med. Chem. Commun., 2018, 9, 282-298.
39 G.M. Morris, R. Huey, W. Lindstrom, M.F. Sanner, R.K. Belew, D.S. Goodsell and A.J. Olson, J. Comput. Chem., 2009, 30, 2785-2791.
40 O.Trott and A. J. Olson, J. Comput. Chem., 2010, 31, 455-461.
41 D. P. Yeggoni, M. Gokara, D. M. Manidhar, A. Rachamallu, S. Nakka, C. S. Reddy and R. Subramanyam, Mol. Pharmaceutics, 2014, 11, 1117-1131.
42 Y. R. Zheng, K. Suntharalingam, T. C. Johnstone, H. Yoo, W. Lin, J. G.Brooks and S. J. Lippard, J. Am. Chem. Soc., 2014, 136: 8790-8798.
43 M.F. Iskander, T.E. Khalil, W. Haase, R. Werner, I. Svoboda and H. Fuess, Polyhedron, 2001, 20, 2787-2798.
44 S. Tabassum, M. Zaki, M. Ahmad, M. Afzal, S. Srivastav, S. Srikrishna and F. Arjmand, Eur. J. Med. Chem., 2014, 83, 141-154.
45 A.M. Merlot, S. Sahni, D.J. Lane, A.M. Fordham, N. Pantarat, D.E. Hibbs, V. Richardson, M.R. Doddareddy, J.A. Ong, M.L. Huang, D.R. Richardson and D.S. Kalinowski, Oncotarget, 2015, 6, 10374-10398.




 

View Article Online
DOI: 10.1039/C8MD00223A



46 Y. Gou, Y. Zhang, J. Qi, S. Chen, Z. Zhou, X. Wu, H. Liang and F. Yang, Oncotarget, 2016, 7, 67004-67019.
47 B.K. Sahoo, K.S. Ghosh and S. Dasgupta, Biopolymers, 2009, 91, 108-119.
48 N. Ibrahim, H. Ibrahim, S. Kim, J.P. Nallet and F. Nepveu, Biomacromolecules, 2010, 11, 3341-3351.
49 Y. Q. Wang, X.Y. Wang, J. Wang, Y. M. Zhao, W. J. He and Z. J. Guo, Inorg. Chem. 2011, 50, 12661-12668.
50 B. P. Espósito and Najjar, R. Coord. Chem. Rev. 2002, 232, 137-149.
51 W. Hu, Q. Luo, K. Wu, X. Li, F. Wang, Y. Chen, X. Ma, J. Wang, J. Liu, S. Xiong and P. J. Sadler, Chem. Commun. 2011, 47, 6006-6008.
52 R. J. Williams, M. Lipowska, G.Patonay and L. Strekowski, Anal. Chem. 1993, 65, 601-605.
53 Y. Gou, J. Li, B. Fan, B. Xu, M. Zhou and F. Yang, Eur. J. Med. Chem., 2017, 134, 207-217.
54 K. Suntharalingam, T.C. Johnstone, P.M. Bruno, W. Lin, M.T. Hemann and S.J. Lippard, J. Am. Chem. Soc., 2013, 135, 14060-14063.
55 Saswati, A. Chakraborty, S. P. Dash, A. K. Panda, R. Acharyya, A. Biswas, S. Mukhopadhyay, S.K. Bhutia, A. Crochet, Y. P. Patil, M. Nethaji and R. Dinda, Dalton Trans., 2015, 44, 6140-6157.
56 M.J. Li, T.Y. Lan, X.H. Cao, H.H. Yang, Y. Shi, C. Yi and G.N. Chen, Dalton Trans., 2014, 43, 2789-2798.
57 G. Ferraro, L. Massai, L. Messori and A. Merlino, Chem. Commun., 2015, 51, 9436-9439.
58 F. Shen, Y.X. Liu, S.M. Li, C.K. Jiang, B.F. Wang, Y.H. Xiong, Z.W. Mao and X.Y. Le, New J. Chem., 2017, 41, 12429-12441.
59 S. Kathiresan, S. Mugesh, J. Annaraj and M. Murugan, New J. Chem., 2017, 41, 1267-1283.
60 B. Wu, P. Dröge and C. A.Davey, Nat. Chem. Biol., 2008, 4(2): 110-112.
61 T. Chen and Y.S. Wong, Cell. Mol. Life Sci., 20018, 65, 2763-2775.
62 P.L. Toogood, Curr. Opin. Chem. Biol., 2002, 6, 472-478.
63 J. Bloom and F.R. Cross, Nat. Rev. Mol. Cell Biol., 2007, 8, 149-160.
64 W. Ginzinger, G. Muhlgassner, V.B. Arion, M.A. Jakupec, A. Roller, M. Galanski, M. Reithofer, W. Berger and B.K. Keppler, J. Med. Chem., 2012, 55, 3398-3413.
65 A. Kisova, L. Zerzankova, A. Habtemariam, P.J. Sadler, V. Brabec and J. Kasparkova, Mol. Pharm., 2011, 8, 949-957.
66 C. Wang and R.J. Youle, Annu. Rev. Genet., 2009, 43, 95-118.
67 L. He, S.Y. Liao, C.P. Tan, R.R. Ye, Y.W. Xu, M. Zhao, L.N. Ji and Z.W. Mao, Chemistry (Easton), 2013, 19, 12152-12160.
68 M.F. van Delft and D.C. Huang, Cell Res., 2006, 16, 203-213.

View Article Online
DOI: 10.1039/C8MD00223A

Three Cu(II) complexes **(C1-C3)**, especially **C3** with the ligand derived from benzocaine exhibited more selective for HeLa cells, and arrested cell cycle, promoted tumor cell apoptosis.